Preprints of the 21st IFAC World Congress (Virtual)
Berlin, Germany, July 12-17, 2020

Fault estimation methods in descriptor system with partially decoupled disturbances. ⋆

Manh-Hung Do * **Damien Koenig** * **Didier Theilliol** **

* *Univ. Grenoble Alpes, CNRS, Grenoble INP, GIPSA-lab, 38000 Grenoble, France.*
(e-mail: {manh-hung.do, damien.koenig}@gipsa-lab.grenoble-inp.fr)
** *University of Lorraine, CRAN, UMR 7039, Campus Sciences, B.P.70239, 54506 Vandoeuvre-les-Nancy Cedex, France.*
(e-mail: didier.theilliol@univ-lorraine.fr)

Abstract: The main contribution of this paper consists of the development of two methods for actuator fault estimation in dealing with the partially decoupled disturbances of the descriptor system, which is divided into decoupled and non-decoupled unknown inputs (UI). Based on the conventional UI observer, both of the solutions decouples the fault estimation with the first group of UI, while the second UI group is handled differently by each method. Finally, a numerical example with comparisons points out the performance of each approach.

Keywords: Unknown Input Observer, $\mathcal{H}_\infty$ synthesis, Descriptor system, Fault estimation, Frequency-shaping filter.

1. INTRODUCTION

Nowadays, the descriptor system, i.e. singular system, plays an important role in both theoretical and practical aspects as it can be used to model a wide range of chemical, mineral, electrical and economic systems (see Dai (1989)). That leads to a great interest dedicated to the analysis, design, and especially fault detection and diagnosis (FDD) techniques, which not only identify faults but also estimate their magnitudes and shapes under the existence of disturbances. The FDD process in the descriptor system is inspired by state estimator, which was realized through the works of Darouach and Boutayeb (1995); Hou and Muller (1999). Then questions concerning the solution for system perturbed by unknown inputs (UI) are placed, which promotes the development of the well-known unknown input (UI) observer in Darouach et al. (1996); Chen et al. (1996); Koenig et al. (2008). By choosing properly a group of parametric matrices that decouple the UI disturbances in state estimation, the dynamics of estimation error is asymptotically stable, i.e. the convergence towards 0. Regarding FDD purpose, a proportional multi-integral UI observer has been introduced in Koenig (2005) by considering the high-order polynomial fault and its derivatives as states of an augmented system. However, one notable drawback associated with this kind of UI observer design is the satisfaction of decoupling and detectability conditions (see Lemma 2 in Koenig (2005)). Consequently, the design of UI observer with partially decoupled disturbances becomes an interesting topic in the research community.

To the best of authors' knowledge, few works such as that of Bezzaoucha et al. (2011) were conducted to handle the above problems in linear systems with partially decoupled disturbances by using the UI observer. In terms of FDD, Xu et al. (2016) and Gao et al. (2016) have presented a novelty of UI-observer. In that design, the disturbances are divided into two main groups: one can be decoupled by choosing the appropriate matrices, and the other contains all non-decoupled disturbances. As a result, the estimation error is now only affected by the group of the second one. In Xu et al. (2016), the fault detection has been realized by using the set-theorem to deal with this non-decoupled group; while for 2^{nd}-order polynomial fault estimation in Gao et al. (2016) the gains of UI observer are calculated to ensure the stability of estimation error dynamics as well as its insensitivity to disturbances by using the $\mathcal{H}_\infty$ synthesis. Despite its performance, those papers are only focused on the special case of the singular matrix ($E = I$) and the $\mathcal{H}_\infty$ performance can be affected when tackling a great amount of non-decoupled UIs. Inspired by this strategy, Liu et al. (2018) introduced an UI observer for the descriptor system generated from system state and fault. However, this solution is implemented only if the initial system is non-singular, not to mention that its existence conditions only concern the new augmented descriptor system instead of the original one. Hence, there is a need to complete this kind of observer design for the descriptor system framework.

For such above reasons in UI observer-based design, authors are motivated to make the following contributions for the FDD process in the UI descriptor system:

- Development of the global $\mathcal{H}_\infty$ approach as an extension result of Gao et al. (2016) with its existence conditions depending directly on the parameters of the initial descriptor system.

⋆ This work is supported by the ITEA3 European Project through EMPHYSIS under Grant 15016.

- A novel approach to overcome the limitation of global $\mathcal{H}_\infty$ solution in handling the non-decoupled UIs, which is resulted from the combination of frequency-shaping filter and the $\mathcal{H}_\infty$ synthesis.

Additionally, a numerical example is presented to demonstrate the approaches. Through the frequency analysis and time simulation, the performance of methods is highlighted.

The paper is organized as follows. Firstly, Section 2 introduces the system representation. To deal with partially decoupled disturbances, the observer design with the two approaches is defined in Section 3 where the proof of detectability condition is provided in the Appendix. Then, a numerical example with comparisons in Section 4 illustrates the performance of each solution. A general discussion on existence conditions of observer and frequency-shaping filter is mentioned in Section 5. Finally, Section 6 concludes the paper.

Notations: $\mathbb{R}^n$ and $\mathbb{R}^{m\times n}$ respectively represent the n-dimensional Euclidean space and the set of all m × n real matrices; X^T is the transpose of the matrix X; 0 and I denote, respectively, the zero and the identity matrix with appropriate dimensions; $X^\dagger$ is the Moore-Penrose inverse of X; the symbol $(*)$ denotes the transposed block in the symmetric position; $\mathcal{R}(x)$ is the real part of the complex number x; $eig(X)$ presents all eigenvalues of matrix X; and we denote $He\{A\} = A + A^T$.

2. PROBLEM FORMULATION

Consider the following descriptor system with faulty actuator:

$$\begin{cases} E\dot{x} &= Ax + Bu + D_w w + Bf \\ y &= Cx \end{cases}, \tag{1}$$

where:

- $x \in \mathbb{R}^{n_x}$ is the state vector; $y \in \mathbb{R}^{n_y}$ is the measurement output vector; $u \in \mathbb{R}^{n_u}$ is the input vector
- $w \in \mathbb{R}^{n_w} = \begin{bmatrix} w_1^T & w_2^T & w_3^T \end{bmatrix}^T$ is the disturbance vector. In which,
  - $w_1 \in \mathbb{R}^{n_{w1}}$ is the UI satisfying decoupling condition in UI observer design.
  - $w_2 \in \mathbb{R}^{n_{w2}}$ is the bounded UI with known bandwidth $[\underline{f_{w_2}}, \overline{f_{w_2}}]$ and does not satisfy decoupling condition in UI observer design.
  - $w_3 \in \mathbb{R}^{n_{w3}}$ is the non-decoupled disturbance with unknown bandwidth.
- $f \in \mathbb{R}^{n_u}$ is the actuator fault vector to be estimated, which can be presented as a polynomial to address a wide range of faults, such as abrupt faults ($\dot{f} = 0$) and incipient faults ($\ddot{f} = 0$) (see Ding (2008)), or even the degradation (see Do et al. (2019)).
$$f(t) = \alpha_0 + \alpha_1 t + \ldots + \alpha_{n-1}t^{n-1} + \alpha_n t^n, \tag{2}$$
where the $(n+1)^{th}$ derivative of f is null (i.e, $f^{(n+1)} = 0$) and α_i $(i = 0, 1, \ldots, n)$ is unknown constant vector.
- Matrices $E, A, B, C,$ $D_w = [D_{w1}\ D_{w2}\ D_{w3}]$ are constant matrices with appropriate dimension.

By considering the derivatives of f as extended states, an augmented system is obtained:

$$\begin{cases} E_a\dot{x}_a = A_a x_a + B_a u + D_{wa} w \\ y = C_a x_a \end{cases}, \tag{3}$$

where $x_a = \begin{bmatrix} x^T & f^T & f^{(1)T} & \ldots & f^{(n-1)T} & f^{(n)T} \end{bmatrix}^T \in \mathbb{R}^{n_{x_a}}$, $n_{x_a} = n_x + (n+1)n_u$, $C_a = [C\ 0\ 0\ \ldots\ 0\ 0]$, $E_a = \begin{bmatrix} E & 0 & 0 & \ldots & 0 & 0 \\ 0 & I & 0 & \ldots & 0 & 0 \\ 0 & 0 & I & \ldots & 0 & 0 \\ \ldots & \ldots & \ldots & \ldots & \ldots & \ldots \\ 0 & 0 & 0 & \ldots & I & 0 \\ 0 & 0 & 0 & \ldots & 0 & I \end{bmatrix}$, $A_a = \begin{bmatrix} A & B & 0 & \ldots & 0 & 0 \\ 0 & 0 & I & \ldots & 0 & 0 \\ 0 & 0 & 0 & \ldots & 0 & 0 \\ \ldots & \ldots & \ldots & \ldots & \ldots & \ldots \\ 0 & 0 & 0 & \ldots & 0 & I \\ 0 & 0 & 0 & 0 & \ldots & 0 \end{bmatrix}$,

$B_a = \begin{bmatrix} B \\ 0 \\ 0 \\ \ldots \\ 0 \\ 0 \end{bmatrix}$, and $D_{wa} = \begin{bmatrix} D_w \\ 0 \\ 0 \\ \ldots \\ 0 \\ 0 \end{bmatrix} = [D_{w1a}\ D_{w2a}\ D_{w3a}]$.

The observer design to estimate fault f under the existence of UI w is presented in the next section.

3. OBSERVER DESIGN

In this section, the UI w_1 of w is decoupled from estimation process by the conventional UI observer-based design, whereas the impact of the UI $w_{23} = \begin{bmatrix} w_2^T & w_3^T \end{bmatrix}^T$ on fault estimation are studied in the two following approaches:

Approach 1: Global $\mathcal{H}_\infty$ attenuation for both non-decoupled UIs w_2 and w_3, similar to the approach suggested by Gao et al. (2016). In which, the existence conditions are derived from the initial descriptor system and observer parameters satisfy the following objectives.

- For $w_{23} = 0$, the estimation error is asymptotically stable.
- For $w_{23} \neq 0$, attenuation of exogenous input w_{23} on the fault estimation error e_f is achieved by minimizing γ_{23} such that:
$$\frac{\|e_f\|_2}{\|w_{23}\|_2} \leq \gamma_{23}, \tag{4}$$

where $e_f = f - \hat{f}$ is fault estimation error and $\hat{f}$ is the estimated fault.

Approach 2: Combination of the frequency-shaping filter and $\mathcal{H}_\infty$ attenuation, where UIs w_2 and w_3 are handled separately:

- UI w_2 is attenuated by a frequency-shaping filter corresponding to its known bandwidth.
- UI w_3 is attenuated by $\mathcal{H}_\infty$ optimization as mentioned in Approach 1. For $w_3 \neq 0$, attenuation of exogenous input w_3 on the fault estimation error e_f is achieved by minimizing γ_3 such that:
$$\frac{\|e_f\|_2}{\|w_3\|_2} \leq \gamma_3. \tag{5}$$

Remark 1: Comparing to **Approach 1**, this method relaxes the number of elements in non-decoupled UI vector used for $\mathcal{H}_\infty$ optimization.

The details on observer design for each approach are presented in subsections 3.1 and 3.2, respectively.

For the existence of observer, the following assumptions are considered:

$$(A.1)\quad \text{rank}\begin{bmatrix} E & D_{w1} \\ C & 0 \end{bmatrix} = n_x + n_{w1}. \tag{6}$$

$$(A.2)\quad \text{rank}\begin{bmatrix} (sE-A) & -B & D_{w1} \\ 0 & sI & 0 \\ C & 0 & 0 \end{bmatrix} = n_x + n_{w1}, \forall \mathcal{R}(s) \geq 0. \tag{7}$$

It is noted that the condition (A.1) corresponds to not only the impulse-free condition of the singular system but also the UI-decoupling condition. Meanwhile, the assumption (A.2) is the condition for R-detectability.

3.1 Approach 1: Global $\mathcal{H}_\infty$ attenuation

The UI observer has the structure (as illustrated in Fig. 1):

$$\begin{cases} \dot{z} = Fz + Gu + Ly \\ \hat{x}_a = z + Ny \\ \hat{f} = C_{af}\hat{x}_a \end{cases}, \tag{8}$$

where $\hat{x}_a = \begin{bmatrix} \hat{x}^T & \hat{f}^T & \hat{f}^{(1)T} & \dots & \hat{f}^{(n-1)T} & \hat{f}^{(n)T} \end{bmatrix}^T$ is the estimated state of x_a in (3); $\hat{f}$ is the estimated fault; and $C_{af} = \begin{bmatrix} 0_{n_u \times n_x} & I_{n_u} & 0_{n_u, n_{xa}-n_x-n_u} \end{bmatrix}$.

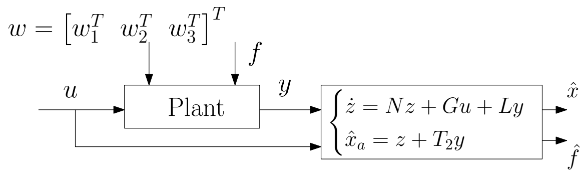

Fig. 1. General scheme of UI observer

Choose $e = x_a - \hat{x}_a$ as the estimation error and suppose that there exists T such that

$$TE_a + NC_a = I, \tag{9}$$

we obtain:

$$e = x_a - z - Ny = TE_a x_a - z. \tag{10}$$

Then, its dynamics is presented as:

$$\begin{aligned} \dot{e} &= TE_a\dot{x}_a - \dot{z} && (11) \\ &= Fe + (TA_a - FTE_a - LC_a)x_a \\ &\quad + (TB_a - G)u + TD_{w1a}w_1 + TD_{w23a}w_{23}, && (12) \end{aligned}$$

where $w_{23} = \begin{bmatrix} w_2^T & w_3^T \end{bmatrix}^T \in \mathbb{R}^{n_{w23}}$, $n_{w23} = n_{w2} + n_{w3}$ and $D_{w23a} = [D_{w2a} \ D_{w3a}]$.

In order for e to be stabilized and decoupled from the UI w_1, the following conditions have to be satisfied:

$$\text{F is Hurwitz, i.e. } \mathcal{R}(eig(F)) < 0, \tag{13}$$
$$TA_a - FTE_a - LC_a = 0, \tag{14}$$
$$G = TB_a, \tag{15}$$
$$TD_{w1a} = 0. \tag{16}$$

From (14), by replacing $TE_a = I - NC_a$ and then choosing $K = L - FN$, it follows that:

$$TA_a - KC_a - F = 0 \tag{17}$$

By combining the three conditions which are $TE_a + NC_a = I$, (16) and (17), we obtain:

$$[T \ N \ K \ F]\,\Theta = \Omega, \tag{18}$$

where $\Omega = \begin{bmatrix} I_{n_{x_a}} & 0_{n_{x_a} \times (n_{x_a}+n_{w1})} \end{bmatrix}$, $\Theta = \begin{bmatrix} E_a & A_a & D_{w1a} \\ C_a & 0 & 0 \\ 0 & -C_a & 0 \\ 0 & -I_{n_{x_a}} & 0 \end{bmatrix}$

The solution of (18) exists if and only if $\text{rank}\begin{bmatrix} \Theta \\ \Omega \end{bmatrix} = \text{rank}(\Theta)$, which is equivalent that Θ is a full-column rank matrix (see Koenig (2005)), i.e. $\text{rank}(\Theta) = 2n_{xa} + n_{w1}$

$$\Leftrightarrow \text{rank}\begin{bmatrix} E_a & D_{w1a} \\ C_a & 0 \end{bmatrix} = n_{xa} + n_{w1}. \tag{19}$$

Replacing the definition of E_a, C_a, and D_{w1a} with matrices of original system (1), a condition which is equivalent to assumption (A.1) is obtained.

Under (A.1), the generalized solution of (18) is given as:

$$[T \ N \ K \ F] = \Omega\Theta^\dagger - Z\Theta^\perp, \tag{20}$$

where $\Theta^\perp = (I - \Theta\Theta^\dagger)$ and Z is an arbitrary matrix.

From (12), (17) and (20), the influence of w_{23} on estimation error $e_f = f - \hat{f}$ is expressed as:

$$\begin{cases} \dot{e} = (TA_a - KC_a)e + TD_{w23a}w_{23} \\ e_f = C_{af}e \end{cases} \tag{21}$$

In other words,

$$\begin{cases} \dot{e} = (\Omega\Theta^\dagger\phi_1 - Z\Theta^\perp\phi_1)e + (\Omega\Theta^\dagger\phi_2 - Z\Theta^\perp\phi_2)w_{23} \\ e_f = C_{af}e \end{cases} \tag{22}$$

where $\phi_1 = \begin{bmatrix} A_a \\ 0_{n_y \times n_{x_a}} \\ -C_a \\ 0_{n_{x_a} \times n_{x_a}} \end{bmatrix}$ and $\phi_2 = \begin{bmatrix} D_{w23a} \\ 0_{(2n_y + n_{x_a}) \times n_{w23}} \end{bmatrix}$.

The above error dynamics can be stabilized thanks to the detectability of the pair $(\Omega\Theta^\dagger\phi_1, \Theta^\perp\phi_1)$ given as the condition below:

$$\text{rank}\begin{bmatrix} sI - \Omega\Theta^\dagger\phi_1 \\ \Theta^\perp\phi_1 \end{bmatrix} = n_{x_a} \quad \forall\ \mathcal{R}(s) \geq 0, \tag{23}$$

which is equivalent to condition (A.2) (proof is easily derived from Appendix of Koenig et al. (2008)). Then, the gain Z satisfying the objective (4) can be found from the following theorem.

Theorem 1. Under (A.1) and (A.2), if there exist a symmetric positive-definite matrix P and a matrix Q which minimize γ_{23} in (4) and satisfy that:

$$\begin{bmatrix} \Gamma & P\Omega\Theta^\dagger\phi_2 + Q\Theta^\perp\phi_2 & C_{af}^T \\ (*) & -\gamma_{23}^2 I & 0 \\ (*) & (*) & -I \end{bmatrix} < 0, \tag{24}$$

with

$$\Gamma = He\{P\Omega\Theta^\dagger\phi_1 + Q\Theta^\perp\phi_1\}, \tag{25}$$

$$\phi_1 = \begin{bmatrix} A_a^T & 0_{n_y \times n_{x_a}}^T & -C_a^T & 0_{n_{x_a} \times n_{x_a}}^T \end{bmatrix}^T, \tag{26}$$

$$\phi_2 = \begin{bmatrix} D_{w23a}^T & 0_{(2n_y + n_{x_a}) \times n_{w23}}^T \end{bmatrix}^T, \tag{27}$$

the estimation error in (22) satisfies the objectives in **Approach 1** with the gain $Z = -QP^{-1}$.

Remark 2: If $E = I$ and the columns of Z corresponding to parametric matrices T and N in (20) are null, the result in Gao et al. (2016) is re-obtained. According to Gao et al. (2016), the parameters T and N are only the basic results of generalized solution, i.e. without the tuning of the arbitrary matrix, thus limiting the freedom of the observer design comparing to that in Theorem 1.

Proof. The sufficient condition for the stability of (22) and attenuation objective (4) is that:

$$\dot{V} + e_f^T e_f - \gamma_{23}^2 w_{23}^T w_{23} < 0. \tag{28}$$

By choosing the Lyapunov function $V = e^T Pe$ and $Q = -PZ$, it follows that:

$$\begin{bmatrix} e^T & w_{23}^T \end{bmatrix} \begin{bmatrix} \Gamma + C_{af}^T C_{af} & P\Omega\Theta^{\dagger}\phi_2 + Q\Theta^{\perp}\phi_2 \\ (*) & -\gamma_{23}^2 I \end{bmatrix} \begin{bmatrix} e \\ w_{23} \end{bmatrix} < 0. \tag{29}$$

The above inequality holds $\forall \begin{bmatrix} e^T & w_{23}^T \end{bmatrix}^T \neq 0$ if:

$$\begin{bmatrix} \Gamma + C_{af}^T C_{af} & P\Omega\Theta^{\dagger}\phi_2 + Q\Theta^{\perp}\phi_2 \\ (*) & -\gamma_{23}^2 I \end{bmatrix} < 0. \tag{30}$$

Applying the Schur complement to above LMI, the condition (24) is obtained, which completes the proof.

The parameters $[T \; N \; K \; F]$ are calculated by replacing values of Z in (20), then $L = K + FN$ and $G = TB_a$.

3.2 Approach 2: Combination of the frequency-shaping filter and $\mathcal{H}_\infty$ attenuation

The aim of UI observer is to decouple the estimation error from disturbances, which is equivalent to a transmission zeros from UIs to the measurement (see Chen et al. (1996)). Based on this idea, to generate similarly the behavior of UI w_2 as that of a possibly-decoupled disturbance, a frequency-shaping filter is implemented to the output y, which characterizes the disturbance attenuation in the known bandwidth $[\underline{f_{w_2}}, \overline{f_{w_2}}]$ of UI w_2. The output $\bar{y}$ of the stable filter Q can be now considered as a new measurement not perturbed by UI w_2. The design process is summarized in Fig. 2

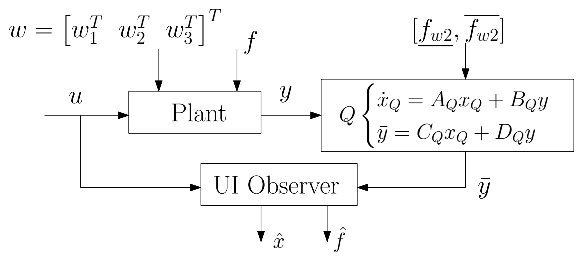

Fig. 2. Frequency-shaping filter implementation for UI observer

The stable filter Q can be expressed as:

$$Q : \begin{cases} \dot{x}_Q = A_Q x_Q + B_Q y \\ \bar{y} = C_Q x_Q + D_Q y \end{cases} \tag{31}$$

where A_Q is Hurwitz.

It yields an augmented system:

$$\begin{cases} \bar{E}_a \dot{\bar{x}}_a & = \bar{A}_a \bar{x}_a + \bar{B}_a u + \bar{D}_{wa} w \\ \bar{y} & = \bar{C}_a \bar{x}_a \end{cases} \tag{32}$$

In which, $\bar{x}_a = \begin{bmatrix} x_a \\ x_Q \end{bmatrix} \in \mathbb{R}^{n_{\bar{x}_a}}$, $\bar{E}_a = \begin{bmatrix} E_a & 0 \\ 0 & I \end{bmatrix}$, $\bar{A}_a = \begin{bmatrix} A_a & 0 \\ B_Q C_a & A_Q \end{bmatrix}$, $\bar{B}_a = \begin{bmatrix} B_a \\ 0 \end{bmatrix}$, $\bar{D}_{wa} = \begin{bmatrix} D_{wa} \\ 0 \end{bmatrix}$, $\bar{C}_a = [D_Q C_a \; C_Q]$.

The observer design for the above system (32) has the same structure as that of conventional UI observer to decouple w_1 while integrating implicitly the frequency-shaping effect for non-decoupled UI w_2:

$$\begin{cases} \dot{z} = \bar{F}z + \bar{G}u + \bar{L}\bar{y} \\ \hat{\bar{x}}_a = z + \bar{N}\bar{y} \\ \hat{f} = \bar{C}_{af}\hat{\bar{x}}_a \end{cases} \tag{33}$$

where $\hat{\bar{x}}_a$ is the estimated state of $\bar{x}_a$ and $\bar{C}_{af} = \begin{bmatrix} 0_{n_u \times n_x} & I_{n_u} & 0_{nu, n_{\bar{x}_a} - n_x - n_u} \end{bmatrix}$.

As Q is a stable filter, the conditions for observer existence (A.1) and (A.2) are also those for augmented system (32). Similarly to **Approach 1**, the following results are obtained:

$$\begin{bmatrix} \bar{T} & \bar{N} & \bar{K} & \bar{F} \end{bmatrix} = \bar{\Omega}\bar{\Theta}^{\dagger} - \bar{Z}\bar{\Theta}^{\perp}, \tag{34}$$

$$\bar{L} = \bar{K} + \bar{F}\bar{N}, \tag{35}$$

$$\bar{G} = \bar{T}\bar{B}_a, \tag{36}$$

where $\bar{\Theta} = \begin{bmatrix} \bar{E}_a & \bar{A}_a & \bar{D}_{w1a} \\ \bar{C}_a & 0 & 0 \\ 0 & -\bar{C}_a & 0 \\ 0 & -I_{n_{\bar{x}_a}} & 0 \end{bmatrix}$ and $\bar{\Omega} = \begin{bmatrix} I_{n_{\bar{x}_a}} & 0 & 0 \end{bmatrix}$.

Due to the implementation of the output filter, the dynamics of observer can be reduced as follows:

$$\begin{cases} \dot{\bar{e}} = (\bar{\Omega}\bar{\Theta}^{\dagger}\bar{\phi}_1 - \bar{Z}\bar{\Theta}^{\perp}\bar{\phi}_1)\bar{e} + (\bar{\Omega}\bar{\Theta}^{\dagger}\bar{\phi}_2 - \bar{Z}\bar{\Theta}^{\perp}\bar{\phi}_2)w_3 \\ e_f = C_{af}\bar{e} \end{cases} \tag{37}$$

where $\bar{e} = \bar{x}_a - \hat{\bar{x}}_a$, $\bar{\phi}_1 = \begin{bmatrix} \bar{A}_a^T & 0_{n_y \times n_{\bar{x}_a}}^T & -\bar{C}_a^T & 0_{n_{\bar{x}_a} \times n_{\bar{x}_a}}^T \end{bmatrix}^T$ and $\bar{\phi}_2 = \begin{bmatrix} \bar{D}_{w3a}^T & 0_{(2n_y + n_{\bar{x}_a}) \times n_{w3}}^T \end{bmatrix}^T$. The gain $\bar{Z}$ is derived from Theorem 2.

Theorem 2. Under (A.1) and (A.2), if there exist a symmetric positive-definite matrix $\bar{P}$ and a matrix $\bar{Q}$ which minimize γ_3 in (5) and satisfy that:

$$\begin{bmatrix} \bar{\Gamma} & \bar{P}\bar{\Omega}\bar{\Theta}^{\dagger}\bar{\phi}_2 + \bar{Q}\bar{\Theta}^{\perp}\bar{\phi}_2 & \bar{C}_{af}^T \\ (*) & -\gamma_3^2 I & 0 \\ (*) & (*) & -I \end{bmatrix} < 0, \tag{38}$$

with

$$\bar{\Gamma} = He\{\bar{P}\bar{\Omega}\bar{\Theta}^{\dagger}\bar{\phi}_1 + \bar{Q}\bar{\Theta}^{\perp}\bar{\phi}_1\}, \tag{39}$$

$$\bar{\phi}_1 = \begin{bmatrix} \bar{A}_a^T & 0_{n_y \times n_{\bar{x}_a}}^T & -\bar{C}_a^T & 0_{n_{\bar{x}_a} \times n_{\bar{x}_a}}^T \end{bmatrix}^T, \tag{40}$$

$$\bar{\phi}_2 = \begin{bmatrix} \bar{D}_{w3a}^T & 0_{(2n_y + n_{\bar{x}_a}) \times n_{w3}}^T \end{bmatrix}^T, \tag{41}$$

the estimation error in (37) satisfies the objectives in **Approach 2** with the gains $\bar{Z} = -\bar{Q}\bar{P}^{-1}$.

This theorem is similar to Theorem 1, so the proof is omitted.

In the next section, the comparison between the two above approaches is conducted to illustrate the performance of each method.

4. NUMERICAL EXAMPLE

4.1 Model Example

The following example is modified from the descriptor system in Darouach et al. (1996):

- Distribution Matrices: $E = \begin{bmatrix} 1 & 0 & 0 & 0 \\ 0 & 1 & 0 & 0 \\ 0 & 0 & 1 & 0 \\ 0 & 0 & 0 & 0 \end{bmatrix}$,

$A = \begin{bmatrix} -1 & 1 & 0 & 0 \\ -1 & 0 & 0 & 1 \\ 0 & -1 & -1 & 0 \\ 0 & 0 & 0 & 1 \end{bmatrix}$, $B = \begin{bmatrix} 0 \\ 0 \\ 1 \\ 1 \end{bmatrix}$, $D_{w1} = \begin{bmatrix} -0.5 \\ 0 \\ 0 \\ 0 \end{bmatrix}$,

$D_{w2} = \begin{bmatrix} 0 \\ 0.4 \\ 0 \\ 0 \end{bmatrix}$, $D_{w3} = \begin{bmatrix} 0 \\ 0.2 \\ 0.1 \\ 0 \end{bmatrix}$, and $C = \begin{bmatrix} 1 & 0 & 0 & 0 \\ 0 & 0 & -1 & 1 \end{bmatrix}$.

- Actuator fault: is supposed to be a 3^{rd} order polynomial (see Fig. 3), so $n = 3$ is chosen for observer design.

$$f = \sum_{i=1}^{n=3} \frac{(-0.21)^i}{i!}(t)^i. \quad (42)$$

Remark 3: The order n of the estimated fault $\hat{f}$ chosen for observer synthesis must be greater or equal to the real order of the existing fault f.

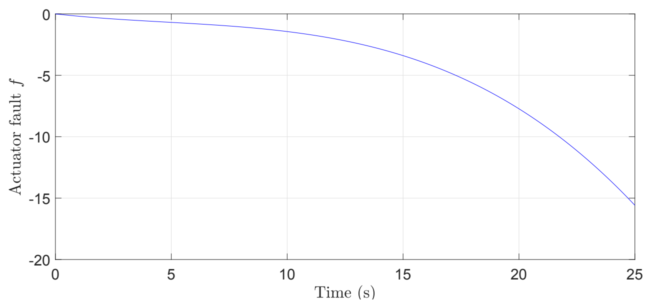

Fig. 3. Actuator fault f

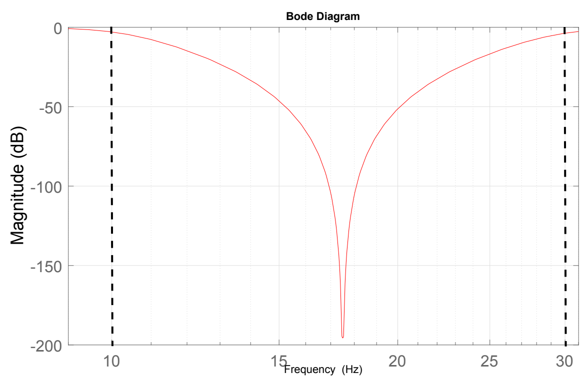

Fig. 4. Output filter

- Frequency bandwidth of UI w_2: $f_{w2} \in [10, 30]$ (Hz). Consequently, the filter Q is designed as a stable 8^{th} order Butterworth-bandstop (see Fig. 4).

4.2 Frequency Analysis

In this part, the frequency behavior of the two approaches in Section 3 are compared. Solving the optimization problem in Theorems 1 and 2 by using Yalmip (see Lofberg (2004)) and Sedumi solver (see Sturm (1999)), the parametric matrices for observer designs in **Approach 1** and **Approach 2** are synthesized. The attenuation level for disturbances in both approaches are presented and compared in the Table 1:

Table 1. Disturbance attenuation Comparison

	Approach 1	**Approach 2**
w_2	$\gamma_{23} = -6.990$ (dB)	Characteristics of filter Q
w_3		$\gamma_3 = -13.978$ (dB)

In Fig. 5, a sudden drop in frequency domain $[10, 30]$ (Hz) expresses the result of filter Q's implementation, as expected from the usage from the frequency-shaping approach.

According to Table 1 and Figs. 5 and 6, by relaxing the size of disturbance vector in $\mathcal{H}_\infty$ synthesis, **Approach 2** gives better attenuation of disturbance influence on estimation error.

4.3 Test Conditions

- Simulation duration: 25 seconds.
- Disturbances:
  - $w_1 = 5sin(2\pi f_{w1})$ with $f_{w1} = 10$ (Hz);
  - $w_2 = 10sin(2\pi f_{w2})$ with $f_{w2} = 17.5$ (Hz) to illustrates clearly the difference in both approaches;
  - $w_3 = 15sin(2\pi f_{w3})$ with $f_{w3} = 35$ (Hz).
- Control input: is chosen as a sinusoidal signal:

$$u = 5sin(2\pi). \quad (43)$$

- System output: is considered not to be perturbed by noise in this study, as described in (1).
- Initial condition: $x_{(0)} = [0.001\ 0\ 0.0020\ 0]^T$, $x_{Q(0)} = 0$, and $\hat{x}_{(0)} = 0$.

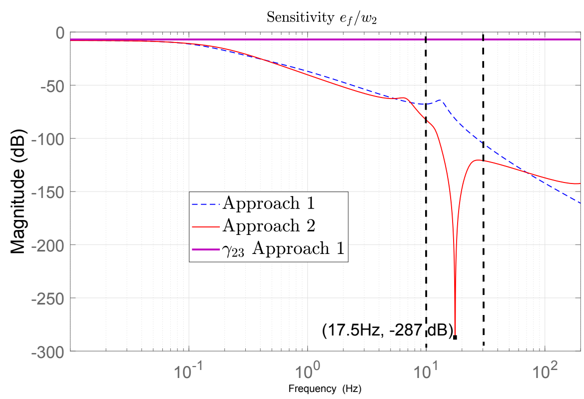

Fig. 5. Sensitivity $|e_f/w_2|$

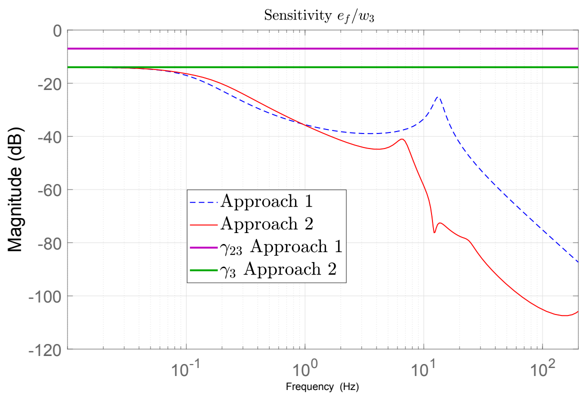

Fig. 6. Sensitivity $|e_f/w_3|$

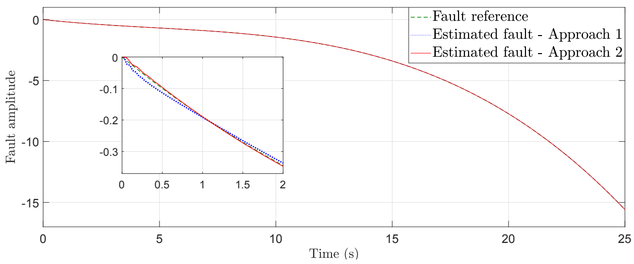

Fig. 7. Fault estimation under influence of w_1

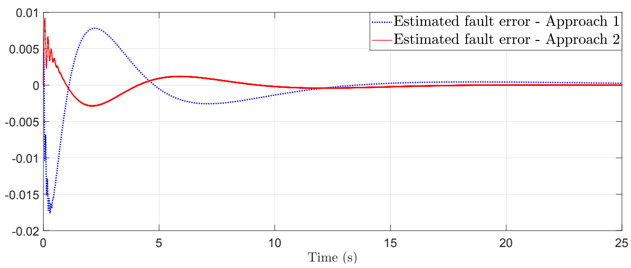

Fig. 8. Estimation error under influence of w_1

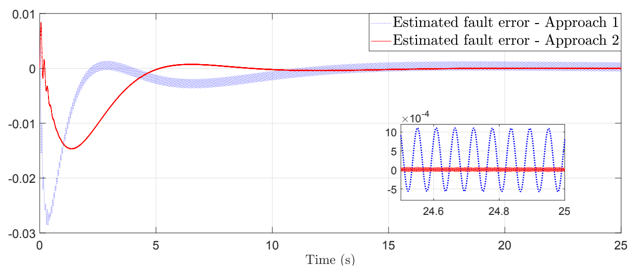

Fig. 9. Estimation error under influence of w_1 and w_2

4.4 Simulation results

Fig. 7 illustrates the estimation of actuator fault through the existence of disturbances, while Figs. 8-10 demonstrate the estimation error. As observed, all fault estimations are converging to fault reference after about 10 seconds, i.e. the estimation error converges towards 0. However, **Approach 1**, i.e. global $\mathcal{H}_\infty$ attenuation method, is more likely to be affected by disturbances w_2 and w_3 comparing to **Approach 2** due to its poor frequency behavior as discussed in subsection 4.2.

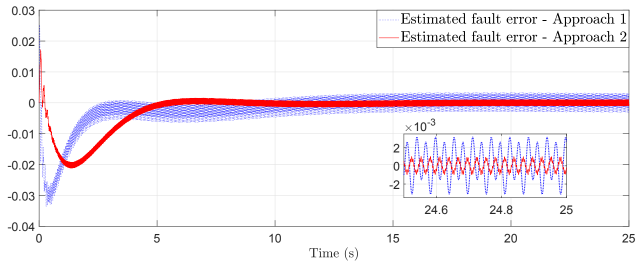

Fig. 10. Fault error under influence of all UIs (w_1, w_2, w_3)

Table 2. RMS of estimation error

Scenarios	**Approach 1**	**Approach 2**
w_1	3.881e-4	2.070e-4
$[w_1, w_2]$	7.008e-4	2.045e-4
$[w_1, w_3]$	18.656e-4	5.952e-4
$[w_1, w_2, w_3]$	19.557e-4	5.941e-4

To evaluate the accuracy of estimation, the root-mean-square value (RMS) of estimation errors is calculated in Table 2. From this comparison, when there is only w_1, the decoupling between the UI w_1 and fault estimation error e_f works correctly as designed in both cases; whereas the differences start to appear in the solutions coping with non-decoupled disturbances. It also proves the better performance of **Approach 2** by treating separately UIs w_2 and w_3, thus relaxing the amount of non-decoupled UIs implemented in $\mathcal{H}_\infty$ synthesis.

5. GENERAL DISCUSSION

5.1 Observer conditions

As noted in (A.1) and (A.2), these assumptions concern only the parameter of possibly-decoupled UI w_1, i.e. D_{w1}, thereby being less restrictive than those of Darouach et al. (1996); Koenig (2005) for all UIs in w, i.e. D_w.

5.2 Frequency-shaping filter implementation

In **Approach 1**, the $\mathcal{H}_\infty$ performance can also be optimized for a specific bandwidth $[\underline{f_{w_2}}, \overline{f_{w_2}}]$ of w_2 by generating a fictive disturbance $\bar{w}_2$ through a weighting function F_w, which is strictly stable and causal (see Koenig et al. (2016)).

The weighting function F_w can be displayed as:

$$F_w : \begin{cases} \dot{x}_w = A_w x_w + B_w \bar{w}_2 \\ w_2 = C_w x_w + D_w \bar{w}_2 \end{cases} . \tag{44}$$

The process is summarized in Fig. 11:

As a result, the system can be rewritten as:

$$\begin{cases} \dot{x}_F &= A_F x_F + B_F u + D_F \bar{w} \\ y &= C_F x_F \end{cases} , \tag{45}$$

where $x_F = \begin{bmatrix} x_a \\ x_w \end{bmatrix}$, $A_F = \begin{bmatrix} A_a & D_{w2a}C_w \\ 0 & A_w \end{bmatrix}$, $B_F = \begin{bmatrix} B_a \\ 0 \end{bmatrix}$, $D_F = \begin{bmatrix} D_{w1a} & D_{w2a}D_w & D_{w3a} \\ 0 & B_w & 0 \end{bmatrix}$, and $C_F = [C_a \ 0]$.

Similarly to **Approach 1**, the objective of observer design for (45) is derived from (4) and is displayed as:

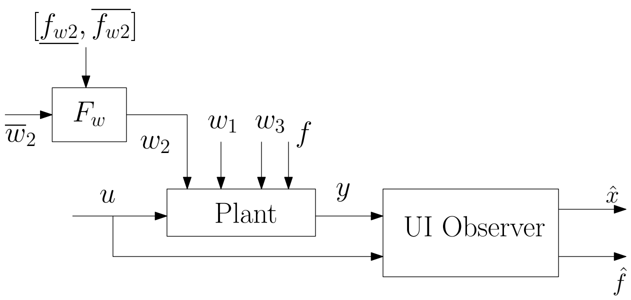

Fig. 11. Weighting function implementation in $\mathcal{H}_\infty$ synthesis.

$$\frac{\|e_f\|_2}{\|\bar{w}_{23}\|_2} \leq \gamma_{23}, \tag{46}$$

where $\bar{w}_{23} = \begin{bmatrix} \bar{w}_2^T & w_3^T \end{bmatrix}^T$.

In other words,

$$\left\{ \begin{array}{l} \dfrac{\|e_f\|_2}{\|\bar{w}_2\|_2} \leq \gamma_{23} \\ \dfrac{\|e_f\|_2}{\|w_3\|_2} \leq \gamma_{23} \end{array} \right. \Leftrightarrow \left\{ \begin{array}{l} \dfrac{\|e_f\|_2}{\|w_2\|_2} \leq \gamma_{23}\|F_w\|^{-1} \\ \dfrac{\|e_f\|_2}{\|w_3\|_2} \leq \gamma_{23} \end{array} \right. \tag{47}$$

Consequently, the influence of the non-decoupled w_2 on fault estimation can be shaped by the choice of inversed filter F_w^{-1}.

Comparing to **Approach 2**, both inversed function F_w^{-1} and frequency-shaping filter Q have the same functionality; however, filter Q only needs to be stable, instead of being simultaneously stable and causal as F_w. Hence, this difference highlights the advantage of the frequency-shaping filter in **Approach 2**. For example, to achieve good attenuation in a narrow bandwidth as that in the numerical example of Section 4, a high-order weighting function F_w^{-1} or frequency-shaping filter Q is required under the form of Butterworth bandstop. In this case, a stable filter Q can be easily designed, whereas the inverse of F_w^{-1}, i.e. F_w is not ensured to be stable.

6. CONCLUSION

In this study, two different approaches which are based on the conventional UI observer to deal with non-decoupled disturbances in the descriptor system have been introduced. The first of which considers the global $\mathcal{H}_\infty$ synthesis for UI impact attenuation, while the other handles the UIs based on the knowledge of their bandwidth. The comparison in fault estimation between the two solutions has highlighted the performance of the proposed separation strategy, where each non-decoupled disturbance is analyzed independently.

For future work, as the problem of partial disturbance in descriptor linear parameter-varying (D-LPV) system has not been broadly studied yet, an extension result of the two above approaches, as well as the impact of frequency-shaping filter on closed-loop performance, can be an interesting topic.

REFERENCES

Bezzaoucha, S., Marx, B., Maquin, D., and Ragot, J. (2011). On the unknown input observer design: a decoupling class approach. In *2011 9th IEEE International Conference on Control and Automation (ICCA)*, 602–607. IEEE.

Chen, J., Patton, R.J., and Zhang, H.Y. (1996). Design of unknown input observers and robust fault detection filters. *International Journal of control*, 63(1), 85–105.

Dai, L. (1989). *Singular control systems*, volume 118. Springer.

Darouach, M. and Boutayeb, M. (1995). Design of observers for descriptor systems. *IEEE transactions on Automatic Control*, 40(7), 1323–1327.

Darouach, M., Zasadzinski, M., and Hayar, M. (1996). Reduced-order observer design for descriptor systems with unknown inputs. *IEEE transactions on automatic control*, 41(7), 1068–1072.

Ding, S.X. (2008). *Model-based fault diagnosis techniques: design schemes, algorithms, and tools*. Springer Science & Business Media.

Do, M.H., Koenig, D., and Theilliol, D. (2019). Robust $\mathcal{H}_2$ observer design for actuator degradation: Application to suspension system. In *2019 4th Conference on Control and Fault Tolerant Systems (SysTol)*. IEEE. doi:10.1109/SYSTOL.2019.8864738.

Gao, Z., Liu, X., and Chen, M.Z. (2016). Unknown input observer-based robust fault estimation for systems corrupted by partially decoupled disturbances. *IEEE Transactions on Industrial Electronics*, 63(4), 2537–2547.

Hou, M. and Muller, P. (1999). Observer design for descriptor systems. *IEEE Transactions on Automatic Control*, 44(1), 164–169.

Koenig, D. (2005). Unknown input proportional multiple-integral observer design for linear descriptor systems: application to state and fault estimation. *IEEE Transactions on Automatic control*, 50(2), 212–217.

Koenig, D., Marx, B., and Jacquet, D. (2008). Unknown input observers for switched nonlinear discrete time descriptor systems. *IEEE Transactions on Automatic Control*, 53(1), 373–379.

Koenig, D., Marx, B., and Varrier, S. (2016). Filtering and fault estimation of descriptor switched systems. *Automatica*, 63, 116–121.

Liu, Y., Wang, Z., and Zhou, D. (2018). State estimation and fault reconstruction with integral measurements under partially decoupled disturbances. *IET Control Theory & Applications*, 12(10), 1520–1526.

Lofberg, J. (2004). YALMIP: A toolbox for modeling and optimization in MATLAB. In *Computer Aided Control Systems Design, 2004 IEEE International Symposium on*, 284–289. IEEE.

Sturm, J.F. (1999). Using sedumi 1.02, a matlab toolbox for optimization over symmetric cones. *Optimization methods and software*, 11(1-4), 625–653.

Xu, F., Tan, J., Wang, X., Puig, V., Liang, B., and Yuan, B. (2016). A novel design of unknown input observers using set-theoretic methods for robust fault detection. In *2016 American Control Conference (ACC)*, 5957–5961. IEEE.